organics

MDPI

Article

Regioselective N- versus P-Deprotonation of Aminophosphane Tungsten(0) Complexes

Tatjana Terschüren [1], Philip Junker [1], Alexander Schmer [1], Arturo Espinosa Ferao [2,*] and Rainer Streubel [1,*]

[1] Institute of Inorganic Chemistry, University of Bonn, Gerhard-Domagk-Str., 1, 53121 Bonn, Germany; t.terschueren@uni-bonn.de (T.T.); philip_junker@gmx.de (P.J.); alexander.schmer@hotmail.de (A.S.)
[2] Departamento de Química Orgánica, Facultad de Química, Campus de Espinardo, Universidad de Murcia, 30100 Murcia, Spain
* Correspondence: artuesp@um.es (A.E.F.); r.streubel@uni-bonn.de (R.S.)

Abstract: 1,2-Bifunctional ligands are rare, in general, which holds especially for those with a P-N linkage. Herein, we report on the synthesis of *P-tert*-butyl substituted aminophosphane $W(CO)_5$ complexes **3a–f** (a: R = R′ = H; b: R = H, R = Me; c: R = H, R′ = ally; d: R = H, R′ = *i*-Pr; e: R = H, R′ = *t*-Bu; f: R = R′ = Me) obtained via formal N-H insertion reactions of Li/Cl phosphinidenoid complex **2** into NH bonds of ammonia and different amines. The 1,2-bifunctionality of **3b** was addressed in targeted regioselective deprotonation reactions leading to amidophosphane complexes **M-4b** or M/N(H)Me phosphinidenoid complexes **M-5b**, respectively (M = Li, K). Remarkable was the observation that reactions of **M-4b** and **M-5b** with MeI as the electrophile resulted in the formation of the same product **7b**. The constitution of all the compounds has been established by means of NMR and IR spectroscopy and mass spectrometry. Two possible reaction pathways were studied in detail using high-level DFT calculations.

Keywords: aminophosphanes; amidophosphanes; 1,2-bifunctional P-ligands; N-deprotonation; P-deprotonation; DFT calculations

check for updates

Citation: Terschüren, T.; Junker, P.; Schmer, A.; Espinosa Ferao, A.; Streubel, R. Regioselective N- versus P-Deprotonation of Aminophosphane Tungsten(0) Complexes. *Organics* **2022**, *3*, 161–172. https://doi.org/10.3390/org3030013

Academic Editor: Tomasz K. Olszewski

Received: 20 April 2022
Accepted: 15 June 2022
Published: 22 June 2022

1. Introduction

The first mention of aminophosphanes **I** (Figure 1) bearing no P-H functionality dates to 1957, when Harris reported the synthesis of $(CF_3)_2$P-NH_2 via the reaction of bis(trifluoromethyl)chlorophosphane with two equivalents of ammonia in the gas phase [1]. Following this, Burg [2] and Smith [3] reported early examples using the aminolysis or treatment of chlorophosphanes with sodium amides. Transition metal complexes **II** with, e.g., iron(0), nickel(0) or molybdenum(0), were first reported in 1971 [4,5]. The synthesis of aminophosphanes **III,** which have a P-H functionality, remained unsuccessful for many years and may be also related to the firm belief that α-elimination under the formation of an amine H-NR_2 and a phosphinidene R-P [6] could occur. Nevertheless, the corresponding complexes of secondary aminophosphanes **IV** have been known since 1975 [6] and have been frequently reported thereafter [7,8]. Two examples of **IV** were obtained from a phosphanido iron(0) complex [9].

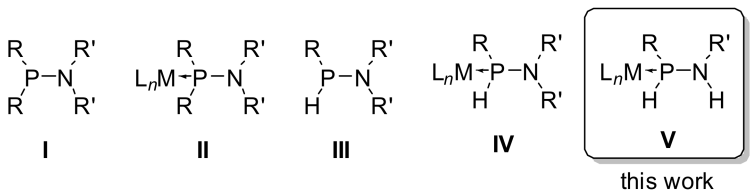

Figure 1. Aminophosphanes **I**, 1,1′-bifunctional aminophosphanes **III** and their complexes **II** and **IV** and 1,2-bifunctional aminophosphane complexes **V** (R, R′ = common organic substituent, M = transition metal, L = ligand).

In 1977, Niecke synthesized the first P-H containing derivative **III**, $(Me_3Si)_2NP(H)$-$NHSiMe_3$ [10], and then the first primary aminophosphane $(Me_3Si)_2N$-PH_2 [11], thus paving the way for further research in various directions. The strategy to use N-H insertion reactions to gain access to aminophosphane complexes of type **II** was first used in 1982 by Mathey [7] and, more recently, by Lammertsma [9]. The alternative use of Li/Cl phosphinidenoid complexes in the formation of aminophosphane complexes of type **IV** was first reported by us in 2012, using the formal N-H insertion [12,13]. The broader scope of this E-H insertion chemistry was reported more recently [14–17] including an overview of formal N-H insertion of Li/X phosphinidenoid complexes [18], adding first examples of **V**, but focusing on sterically demanding substituents, such as triphenylmethyl and bis(trimethylsilyl)methyl, together with $W(CO)_5$ and $Fe(CO)_4$ metal fragments [12–19]. Studies on the chemistry of 1,1′-bifunctional aminophosphane complexes **V** included reactions targeting the P–N bond with hydrogen halides [7] and the P–H bond via deprotonation [12–18]. The latter has resulted in new M/NR'_2 phosphinidenoid complexes if the P-H deprotonation takes place. In contrast, the new 1,2-bifunctionality, i.e., the presence of a P–H and N–H bond, has allowed for initial investigations concerning N-functionalization and/or P/N bifunctional nucleophilicity, thus enabling to form three-membered P-heterocyclic ligands, if sterically demanding P-substituents were used [16].

Herein, 1,2-bifunctional aminophosphane complexes **V** were synthesized, bearing the sterically less demanding *tert*-butyl group [20], and used to address the quest for selective deprotonation and N- vs. P-functionalization. The latter part was also studied in great detail using DFT calculations.

2. Materials and Methods

General experimental details. The syntheses of all compounds were performed under an argon atmosphere using Schlenk techniques and dry solvents. Tetrahydrofuran (THF), diethyl ether, petroleum ether (PE) and *n*-pentane were dried over sodium wire/benzophenone, dichloromethane over calcium hydride and toluene over sodium and further purified by subsequent distillation. All NMR spectra were recorded on a Bruker AV I 300 (300.1 MHz for ^{1}H, 75.5 MHz for ^{13}C; 121.5 MHz for ^{31}P), Bruker AV I 400 (400.1 MHz for 1H, 100.6 MHz for ^{13}C; 162.0 MHz for ^{31}P) and Bruker AV III HD Prodigy 500 (500.2 MHz for ^{1}H, 125.8 MHz for ^{13}C and 202.5 MHz for ^{31}P) spectrometers at 25 °C. The ^{1}H and ^{13}C NMR spectra were referenced to the residual proton resonances and the ^{13}C NMR signals of the deuterated solvents and ^{31}P NMR spectra were referenced to 85% H_3PO_4 as external standards, respectively. Elemental analyses were carried out on a Vario EL gas chromatograph. Mass spectrometric data were collected on a micrOTOF-Q Bruker Daltonik TOF mass spectrometer (ESI, ACPI) or a MAT 90 Thermo Finnigan sector instrument (EI). IR spectra of all compounds were recorded on a Thermo Nicolet 380 FT-IR spectrometer with an attenuated total reflection (ATR) attachment or a Bruker Alpha Diamond ATR FTIR spectrometer.

Complex **1** was prepared according to the literature [21].

General protocol for the synthesis of aminophosphane complexes 3a-e. In a Schlenk tube [{*tert*-butyl(dichloro)phosphane-*κ*P}pentacarbonyltungsten(0)], 1 (1.00 equiv.) was dissolved in THF (25 mmol/L) and 12-crown-4 (1.00 equiv.) was added at ambient temperature to the slightly yellow solution. After cooling to −100 °C and addition of *t*-BuLi (1.7 M in *n*-hexane, 1.10 equiv.), the corresponding amine or ammonia (NH_3: 0.5 M in THF, $MeNH_2$: 2 M in THF) (2.00 (**3a,b,d**) or 3.00 equiv. (**3c,e**)) was added dropwise within 5 min. The yellow solution, later suspension, is left to warm up to −20 °C and after completion of the reaction (monitored by ^{31}P NMR spectroscopy), all volatiles were removed in vacuo ($\approx 1 \cdot 10^{-2}$ mbar). The yellow residue is extracted three times with 10 mL of *n*-pentane (**3a,b,d**) or diethyl ether (**3c**) each. After removal of the solvent under reduced pressure ($\approx 1 \cdot 10^{-2}$ mbar), a yellow to red oil was obtained.

[{Amino(*tert*-butyl)phosphane-*κ*P}pentacarbonyltungsten(0)] (3a). Yield: 214 mg (0.50 mmol, 53%), yellow oil. ^{1}H NMR (500.1 MHz, 298 K, C_6D_6): δ/ppm = 0.71 (d,

$^{3}J_{P,H}$ = 16.9 Hz, 9H, C(CH_3)$_3$), 1.15–1.29 (m, 2H, NH_2), 5.41 (dt, $^{1}J_{P,H}$ = 336.3 Hz, $^{3}J_{H,H}$ = 4.0 Hz, 1H, PH). ^{13}C NMR (125.8 MHz, 298 K, C_6D_6): δ/ppm = 25.0 (d, $^{2}J_{P,C}$ = 7.1 Hz, C(CH_3)$_3$), 32.6 (d, $^{1}J_{P,C}$ = 33.7 Hz, C(CH$_3$)$_3$), 197.0 (d$_{sat}$, $^{1}J_{W,C}$ = 124.6 Hz, $^{2}J_{P,C}$ = 7.3 Hz, *cis*-CO), 199.1 (d$_{sat}$, $^{1}J_{W,C}$ = 143.2 Hz, $^{2}J_{P,C}$ = 21.9 Hz, *trans*-CO). ^{31}P NMR (202.5 MHz, 298 K, C_6D_6): δ/ppm = 47.2 (ddq$_{sat}$, $^{1}J_{W,P}$ = 241.3 Hz, $^{1}J_{P,H}$ = 336.3 Hz, $^{1}J_{P,C}$ = 33.7 Hz, $^{3}J_{P,H}$ = 16.9 Hz). IR (ATR) $\widetilde{\nu}$/cm^{-1} = 3476 (w, ν(NH)), 3384 (w, ν(NH)), 2289 (w, ν(PH)), 2071 (vs, ν(CO)), 1886 (s, ν(CO)) 1556 (s, δ(NH)). MS calcd. for $C_9H_{12}NO_5PW$: 429.0; found (EI) m/z = 428.9. $C_9H_{12}NO_5PW$ (429.01): calcd. C 25.20, H 2.82 N 3.26; found C 28.23 H 3.53 N 3.03.

[{*Tert*-butyl(methylamino)phosphane-κP}pentacarbonyltungsten(0)] (3b). Yield: 627 mg (1.42 mmol, 69%), orange oil. ^{1}H NMR (500.1 MHz, 298 K, C_6D_6): δ/ppm = 0.80 (d, $^{3}J_{P,H}$ = 16.5 Hz, 9H, C(CH_3)$_3$), 0.85 (br m, 1H, NH), 2.09 (dd, $^{3}J_{P,H}$ = 5.7 Hz, $^{3}J_{H,H}$ = 10.6 Hz, 3H, CH_3), 5.41 (dd, $^{1}J_{P,H}$ = 337.9 Hz, $^{3}J_{H,H}$ = 5.2 Hz, 1H, PH). ^{13}C NMR (125.8 MHz, 298 K, C_6D_6): δ/ppm = 26.1 (d, $^{2}J_{P,C}$ = 7.1 Hz, C(CH_3)$_3$), 35.6 (d, $^{1}J_{P,C}$ = 28.3 Hz, C(CH$_3$)$_3$), 36.6 (d, $^{2}J_{P,C}$ = 7.1 Hz, CH_3), 197.3 (d$_{sat}$, $^{1}J_{W,C}$ = 124.8 Hz, $^{2}J_{P,C}$ = 7.2 Hz, *cis*-CO), 199.3 (d$_{sat}$, $^{1}J_{W,C}$ = 143.8 Hz, $^{2}J_{P,C}$ = 21.9 Hz, *trans*-CO). ^{31}P NMR (202.5 MHz, 298 K, C_6D_6): δ/ppm = 68.5 (dm$_{sat}$, $^{1}J_{W,P}$ = 239.1 Hz, $^{1}J_{P,H}$ = 337.9 Hz). IR (ATR) $\widetilde{\nu}$/cm^{-1} = 3436 (w, ν(NH)), 2286 (w, ν(PH)), 2070 (vs, ν(CO)), 1980 (w, ν(CO)), 1887 (s, ν(CO)). MS calcd. for $C_{10}H_{14}NO_5PW$: 443.0; found (EI) m/z = 443.0. $C_{10}H_{14}NO_5PW$ (443.04): calcd. C 27.11, H 3.19 N 3.16; found C 26.70 H 3.22 N 3.11.

[{*Tert*-butyl(allylamino)phosphane-κP}pentacarbonyltungsten(0)] (3c). Yield: 388 mg (0.827 mmol, 80%), orange oil. ^{1}H NMR (500.1 MHz, 298 K, C_6D_6): δ/ppm = 0.81 (d, $^{3}J_{P,H}$ = 16.7 Hz, 9H, C(CH_3)$_3$), 1.19 (br s, 1H, NH), 3.09 (m, 2H, NCH_2CHCH_2), 4.89 (dd, $^{3}J_{H,H}$ = 10.2 Hz, $^{4}J_{H,H}$ = 1.5 Hz, 1H, NCH_2CHCH$_2$), 4.93 (dd, $^{3}J_{H,H}$ = 17.1 Hz, $^{4}J_{H,H}$ = 1.6 Hz, 1H, NCH_2CHCH$_2$), 5.49 (ddt, $^{2}J_{H,H}$ = 17.1 Hz, $^{3}J_{H,H}$ = 10.6 Hz, $^{3}J_{H,H}$ = 5.5 Hz, 1H, NCH_2CHCH$_2$), 5.52 (dd, $^{1}J_{P,H}$ = 339.4 Hz, $^{3}J_{H,H}$ = 5.31 Hz, 1H, PH). ^{13}C NMR (125.8 MHz, 298 K, C_6D_6): δ/ppm = 26.0 (d, $^{2}J_{P,C}$ = 7.2 Hz, C(CH_3)$_3$), 35.7 (d, $^{1}J_{P,C}$ = 28.3 Hz, C(CH$_3$)$_3$), 52.6 (d, $^{2}J_{P,C}$ = 7.0 Hz, NCH_2CHCH$_2$), 115.8 (s, NCH$_2$CHCH_2), 136.3 (d, $^{3}J_{P,C}$ = 4.2 Hz, CH$_2$CHCH$_2$), 197.3 (d$_{sat}$, $^{1}J_{W,C}$ = 124.9 Hz, $^{2}J_{P,C}$ = 7.2 Hz, *cis*-CO), 199.1 (d$_{sat}$, $^{1}J_{W,C}$ = 142.9 Hz, $^{2}J_{P,C}$ = 22.1 Hz, *trans*-CO). ^{31}P NMR (202.5 MHz, 298 K, C_6D_6): δ/ppm = 62.8 (dm$_{sat}$, $^{1}J_{W,P}$ = 240.2 Hz, $^{1}J_{P,H}$ = 339.4 Hz). IR (ATR) $\widetilde{\nu}$/cm^{-1} = 3421 (w, ν(NH)), 2294 (w, ν(PH)), 2070 (vs, ν(CO)), 1979 (w, ν(CO)), 1890 (s, ν(CO)). MS calcd. for [$C_{12}H_{17}NO_5PW$ + H+] 470.1; found (APCI) m/z = 470.0. $C_{10}H_{14}NO_5PW$ (469.03): calcd. C 30.73, H 3.44 N 2.99; found C 31.93 H 3.88 N 2.56.

[{*Tert*-butyl(*iso*-propylamino)phosphane-κP}pentacarbonyltungsten(0)] (3d). Yield: 1.27 g (2.70 mmol, 69%), red oil. ^{1}H NMR (400.1 MHz, 298 K, C_6D_6): δ/ppm = 0.73 (d, $^{3}J_{H,H}$ = 6.4 Hz, 3H, CH(CH_3)$_2$), 0.82 (d, $^{3}J_{H,H}$ = 6.3 Hz, 3H, CH(CH_3)$_2$), 0.85 (d, $^{3}J_{P,H}$ = 16.8 Hz, 9H, C(CH_3)$_3$), 0.95 (m, 1H, NH), 2.74 (m, 1H, CH), 5.58 (dd, $^{1}J_{P,H}$ = 334.0 Hz, $^{3}J_{H,H}$ = 4.7 Hz, 1H, PH). ^{13}C NMR (100.6 MHz, 298 K, C_6D_6): δ/ppm = 25.0 (d, $^{3}J_{P,C}$ = 2.2 Hz, CH(CH_3)$_2$), 25.2 (d, $^{3}J_{P,C}$ = 4.9 Hz, CH(CH_3)$_2$) 25.9 (d, $^{2}J_{P,C}$ = 7.1 Hz, C(CH_3)$_3$), 35.1 (d, $^{1}J_{P,C}$ = 30.7 Hz, C(CH$_3$)$_3$), 51.7 (d, $^{2}J_{P,C}$ = 7.9 Hz, CH(CH$_3$)$_2$), 197.4 (d$_{sat}$, $^{1}J_{W,C}$ = 124.8 Hz, $^{2}J_{P,C}$ = 7.3 Hz, *cis*-CO), 199.2 (d$_{sat}$, $^{1}J_{W,C}$ = 143.3 Hz, $^{2}J_{P,C}$ = 21.9 Hz, *trans*-CO). ^{31}P NMR (162.0 MHz, 298 K, C_6D_6): δ/ppm = 55.8 (dm$_{sat}$, $^{1}J_{W,P}$ = 238.5 Hz, $^{1}J_{P,H}$ = 334.0 Hz). IR (ATR) $\widetilde{\nu}$/cm^{-1} = 3397 (w, ν(NH), 2289 (w, ν(PH)), 2080 (s, ν(CO)), 1914 (vs, ν(CO)). MS calcd. for [$C_{12}H_{18}NO_5PW$] 471.0; found (EI) m/z = 471.1.

[{*Tert*-butyl(*tert*-butylamino)phosphane-κP}pentacarbonyltungsten(0)] (3e). ^{31}P NMR (121.5 MHz, 298 K, THF): δ/ppm = 37.1 (dm$_{sat}$, $^{1}J_{W,P}$ = 239.9 Hz, $^{1}J_{P,H}$ = 340.6 Hz).

[{*Tert*-butyl(dimethylamino)phosphane-κP}pentacarbonyltungsten(0)] (3f). In a 200 mL Schlenk tube, 1.01 g (2.09 mmol, 1.00 equiv.) of **1** are dissolved in 84 mL of THF and 365 µL (2.09 mmol, 1.00 equiv.) of 12-crown-4 are added to the slightly yellow solution. After cooling to −100 °C and addition of 1.3 mL (2.29 mmol, 1.10 equiv.) of *t*-BuLi (1.7 M in *n*-hexane), 3.1 mL (6.26 mmol, 3.00 equiv.) of Me_2NH (2 M in THF) are added dropwise within 5 min. The yellow solution, later suspension, is left to warm up to −20 °C and the solvent is removed in vacuo ($\approx 1 \cdot 10^{-2}$ mbar). The yellow-orange residue is extracted

three times with 25 mL *n*-pentane each. After removal of the solvent under reduced pressure ($\approx 1 \cdot 10^{-2}$ mbar), the orange residue is worked up by column chromatography (Al2O3, h = 5.5 cm, ø = 3 cm, 30 mL PE (40/65), 50 mL PE (40/65):Et_2O = 9:1, 20 mL PE (40/65):Et_2O = 4:1, 80 mL PE (40/65):Et_2O = 1:1). The solvent is removed in vacuo ($\approx 1 \cdot 10^{-2}$ mbar), yielding an orange oil that contains 88% of the product by NMR integration. Orange oil. ^{1}H NMR (500.1 MHz, 298 K, C_6D_6): δ/ppm = 0.87 (d, $^3J_{P,H}$ = 16.0 Hz, 9H, C(CH_3)$_3$), 2.38 (d, $^3J_{P,H}$ = 9.1 Hz, 6H, N(CH_3)$_2$), 5.87 (d, $^1J_{P,H}$ = 346.8 Hz, 1H, PH). ^{31}P NMR (202.5 MHz, 298 K, C_6D_6): δ/ppm = 91.4 ppm (dm$_{sat}$, $^1J_{W,P}$ = 239.9 Hz, $^1J_{P,H}$ = 346.8 Hz). MS calcd. for [$C_{11}H_{16}NO_5PW$ + H+] 458.0; found (ESI(+)) m/z = 458.0.

Lithium[{*tert*-butyl(methylamido)phosphane-κP}pentacarbonyltungsten(0)] (Li-4b). In a 50 mL Schlenk tube, 202.2 mg (0.46 mmol, 1.00 equiv.) of **3b** are dissolved in 18 mL of THF and after cooling to −80 °C, 0.37 mL (0.91 mmol, 1.00 equiv.) of *n*-BuLi (2.5 M in *n*-hexane) are added to the slightly yellow solution. The light-yellow suspension is left to warm up to room temperature and stirred overnight and the solvent is removed in vacuo ($\approx 3 \cdot 10^{-2}$ mbar). The orange residue is washed with 7 mL of PE 65/40 and 0.5 mL of Et_2O twice and twice with 7 mL of PE 65/40. After removal of the solvent under reduced pressure ($\approx 3 \cdot 10^{-2}$ mbar), a yellow-orange solid is obtained. Yield: decomposition before determination, yellow solid. ^{1}H NMR (300.1 MHz, 298 K, THF-d$_8$): δ/ppm = 1.26 (d, $^3J_{P,H}$ = 15.8 Hz, 9H, C(CH_3)$_3$), 2.67 (d, $^3J_{P,H}$ = 6.0 Hz, 3H, NCH_3), 5.78 (d, $^1J_{P,H}$ = 311.0 Hz, 1H, PH). ^{13}C NMR (75.5 MHz, 298 K, THF-d$_8$): δ/ppm = 27.9 (d, $^2J_{P,C}$ = 8.4 Hz, C(CH_3)$_3$), 31.2 (d, $^2J_{P,C}$ = 7.8 Hz, CH_3), 32.6 (d, $^1J_{P,C}$ = 20.8 Hz, *C*(CH_3)$_3$), 209.6 (d, $^2J_{P,C}$ = 8.3 Hz, *cis*-CO), 216.6 (d, $^2J_{P,C}$ = 26.7 Hz, *trans*-CO). ^{31}P NMR (121.5 MHz, 298 K, THF-d$_8$): δ/ppm = 49.2 (dm$_{sat}$, $^1J_{W,P}$ = 188.4 Hz, $^1J_{P,H}$ = 311.0 Hz). IR (ATR) $\widetilde{\nu}$/cm^{-1} = 2070 (vs, ν(CO)), 1906 (s, ν(CO)). MS calcd. for [$C_{10}H_{13}LiNO_5PW$–Li+ + 2H+]: 444.0; found (EI) m/z = 444.0.

[Lithium(12-crown-4)][{*tert*-buty(methylamino)phosphanid-κP}pentacarbonyltungsten(0)] (Li-5b). In a 10 mL Schlenk tube, 38.5 mg (0.087 mmol, 1.00 equiv.) of **3b** are dissolved in 3.5 mL of THF. After adding 30.5 µL (0.17 mmol, 2.00 equiv.) of 12-crown-4 and cooling to −80 °C, 0.07 mL (0.17 mmol, 2.00 equiv.) of *n*-BuLi (2.5 M in *n*-hexane) are added while stirring. From the light yellow reaction solution, an NMR sample is taken after 30 min. ^{31}P NMR (121.5 MHz, 298 K, THF): δ/ppm = 89.9 (broad s).

[Potassium(18-crown-6)][{*tert*-buty(methylamino)phosphanid-κP}pentacarbonyltungsten(0)] (K-5b). In a 10 mL Schlenk tube, 45.0 mg (0.10 mmol, 1.00 equiv.) of **3b** and 53.7 mg (0.20 mmol, 2.00 equiv.) of 18-crown-6 are dissolved in 1.5 mL of THF. After cooling to −80 °C, 40.5 mg (0.20 mmol, 2.00 equiv.) are dissolved in 2.5 mL of THF and are added while stirring. From the light yellow reaction solution, an NMR sample is taken after 30 min. ^{31}P NMR (121.5 MHz, 298 K, THF): δ/ppm = 89.9 (broad s).

[{*Tert*-butyl(methyl)(methylamino)phosphane-κP}pentacarbonyltungsten(0)] (7b). In a 50 mL Schlenk tube, 104 mg (0.235 mmol, 1.00 equiv.) of **3b** are dissolved in 9.4 mL of THF and 83 µL (0.470 mmol, 2.00 equiv.) of 12-crown-4 are added to the slightly yellow solution. After cooling to −80 °C and addition of 0.19 mL (0.470 mmol, 2.00 equiv.) of *n*-BuLi (2.5 M in *n*-hexane), 29 µL (0.470 mmol, 2.00 equiv.) of MeI are added dropwise within 5 min. The light-yellow suspension is to left warm up to room temperature and the solvent is removed in vacuo ($\approx 1 \cdot 10^{-2}$ mbar). The yellow residue is extracted three times with 5 mL *n*-pentane each. After removal of the solvent under reduced pressure ($\approx 1 \cdot 10^{-2}$ mbar), a yellow-orange oil is obtained. Yield: not determined due to 12-crown-4 present, yellow oil. ^{1}H NMR (500.1 MHz, 298 K, C_6D_6): δ/ppm = 0.77 (d, $^3J_{P,H}$ = 15.0 Hz, 9H, C(CH_3)$_3$), 0.81 (br s, 1H, NH) 1.18 (d, $^2J_{P,H}$ = 5.4 Hz, 3H, PCH_3), 2.08 (dd, $^3J_{P,H}$ = 5.7 Hz, $^3J_{H,H}$ = 11.0 Hz, 3H, NCH_3), 3.49 (s, nH, 12-c-4). ^{13}C NMR (125.8 MHz, 298 K, C_6D_6): δ/ppm = 25.4 (d, $^2J_{P;C}$ = 6.7 Hz, C(CH_3)$_3$), 36.2 (d, $^1J_{P,C}$ = 24.2 Hz, *C*(CH_3)$_3$), 36.6 (d, $^2J_{P,C}$ = 7.1 Hz, *C*H_3), 198.2 (dsat, $^1J_{W,C}$ = 125.1 Hz, $^2J_{P,C}$ = 7.5 Hz, *cis*-CO), 199.6 (d$_{sat}$, $^1J_{W,C}$ = 141.8 Hz, $^2J_{P,C}$ = 21.5 Hz, *trans*-CO). ^{31}P NMR (202.5 MHz, 298 K, C_6D_6): δ/ppm = 70.7 (m$_{sat}$, $^1J_{W,P}$ = 252.0 Hz). IR (ATR) $\widetilde{\nu}$/cm^{-1} = 3440 (w, ν(NH)), 2067 (vs,

ν(CO)), 1975 (w, ν(CO)), 1892 (s, ν(CO)). MS calcd. for $C_{11}H_{16}NO_5PW$: 457.0; found (EI) m/z = 456.9.

Computational details. The quantum chemical DFT calculations have been performed with ORCA 4.2.1 [22]. The structures are fully optimized at the TPSS-D3/def2-TZVP + CPCM(THF) level of theory, which combines the TPSS [23] meta-GGA density functional with the BJ-damped DFT-D3 dispersion correction [24,25] and the def2-TZVP basis set [26,27], using the conductor-like screening model (CPCM) continuum solvation model [26–28] for THF solvent (dielectric constant ε = 7.58 and solvent radius R_{solv} = 3.18 Å). The density-fitting RI-J approach [26,29,30] is used to accelerate the geometry optimization and numerical harmonic frequency calculations [31] in solution. The optimized structures are characterized by frequency analysis to identify the nature of located stationary points (no imaginary frequency for true minima and only one imaginary frequency for transition states). Single-point calculations were performed at the hybrid-meta-GGA PW6B95-D3 [32] level using a larger def2-QZVP basis set [27,28]. To help experimental ^{31}P NMR assignment, nuclear magnetic shielding constants for various P-containing complexes are also computed using the GIAO (gauge including atomic orbital) method at the TPSS/def2-QZVP level [33]; the final ^{31}P NMR chemical shifts are computed using the known ^{31}P NMR signal of the complex **3b** [$W(CO)_5P^tBu(H)NHMe$)] at 67.3 ppm in C_6D_6 solution as a reference.

3. Results and Discussion

3.1. Synthesis and Characterization of P–tert–Bu Substituted Aminophosphane Complexes

According to Tolman's cone angle concept extrapolated from phosphine ligands to the organyl R substituent attached to P in computed (PBEh-3c level) R-PCl_2-$W(CO)_5$ compounds **1**, the estimated cone angle for the trityl group (Θ = 178.4°) reveals a much higher steric protection at P than the *t*-Bu group (Θ = 143.5°) [34,35]. The addition of *t*-BuLi to a THF solution of dichloro(*tert*-butyl)phosphane complex **1** in the presence of 12-crown-4 at −100 °C generated the Li/Cl phosphinidenoid complex **2** [34,35], which reacted with ammonia and different amines (Scheme 1). Formal N-H insertion reactions led to the formation of 1,1′-bifuntional aminophosphane $W(CO)_5$ complexes **3a**–**f** (Scheme 1, Table 1).

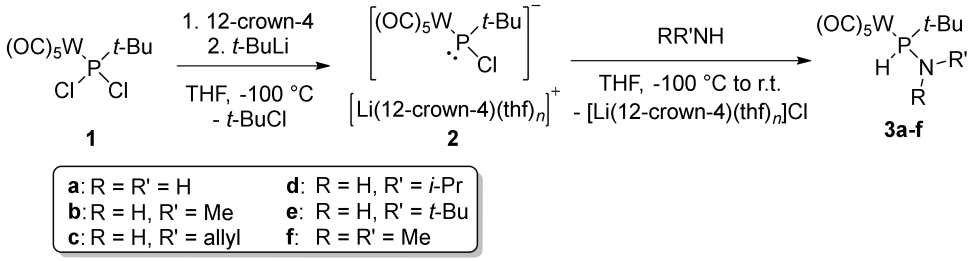

Scheme 1. Synthesis of aminophosphane complexes **3a**–**f** via Li/Cl phosphinidenoid complex **2**.

Table 1. Selected NMR data in THF and yields of synthesized aminophosphane complexes **3a**–**f**.

	R	R′	$\delta(^{31}P)$/ppm	$^1J_{W,P}$/Hz	$^1J_{P,H}$/Hz	yield/%
3a	H	H	45.7	239.0	333.5	56
3b	H	Me	67.3	238.2	337.0	69
3c	H	Allyl	61.6	239.0	339.4	80
3d	H	*i*-Pr	55.5	238.5	334.0	69
3e	H	*t*-Bu	37.1	239.9	340.6	-
3f	Me	Me	91.0	239.5	358.8	-

Highly selective reactions were observed in case of derivatives **3a**–**d**, which were isolated as yellow to red oils in moderate to good yields (Table 1). In the case of **3e** and **3f,** the desired products could be detected only by ^{31}P NMR; hence, **3f** was only partly characterized in an inseparable mixture containing 88% of **3f**.

Surprisingly, the reactions of **2** with other primary and secondary amines, such as ethyl amine, aniline or diethyl amine, did not yield the desired products but an inseparable mixture of compounds, which were not further characterized. In comparison to, e.g., the CPh_3-substituent, the *tert*-butyl substituent exerts a reduced steric shielding onto the phosphorus centre according to Tolman's cone angle concept [20]. This makes this finding particularly astonishing, as a lesser steric shielding onto the phosphorus centre should allow for these reactions to happen, especially as the same reactions had proceeded selectively for the P-CPh_3 substituted analogue of complex **2** [16].

The ^{31}P NMR resonance signals of complexes **3a**–**f** were observed in the range of 37 to 91 ppm and are highfield-shifted compared to the starting material **1**. The analogous *P*-CPh_3 substituted complexes are 5–10 ppm highfield-shifted [15,16], indicating that the *tert*-butyl substituent leads to a slightly lower shielding of the P nucleus. Two substituents at the nitrogen centre shift the resonance to the downfield region. The observed $^1J_{W,P}$ and $^1J_{P,H}$ coupling constants of **3a**–**f** are of similar magnitude, as expected from related derivatives [12,13,15–17].

The FT-IR spectra of **3a** displays the asymmetric and symmetric NH_2 vibration modes at 3476 cm^{-1} and 3384 cm^{-1}, while the bending vibration mode is found at 1556 cm^{-1}. Complexes **3b**–**d** show their N–H bond vibration modes between 3436 cm^{-1} and 3421 cm^{-1}. An unscaled value of 3479 cm^{-1} was computed for **3b** at the working level of theory (see Computational Details). The values for the stretching vibrations are slightly higher than for known complexes, e.g., the *P*-CPh_3 substituted derivatives, which display values at 3400 cm^{-1} to 3350 cm^{-1}. The absorption bands due to P-H vibration modes are measured at about 2290 cm^{-1} with only slight variations in all complexes **3a**–**f**.

3.2. Regioselective Deprotonation of 1,2-Bifunctional Aminophosphane Complexes

Compared to *P*-CPh_3 or *P*-$CH(SiMe_3)_2$ derivatives, the *tert*-Bu substituent seemed to have a clear influence on the outcome of otherwise feasible reactions. Therefore, the quest of regioselective deprotonation of 1,2-bifunctional aminophosphane complexes **3a**–**f** emerged. Previous deprotonation studies of the related, but sterically more demanding, 1,2-bifunctional complexes have shown that one equivalent of base is sufficient, in the presence of a crown ether, to achieve full conversion to the M/N(H)R' phosphinidenoid complex [12,13,15–17]. To study the system in hand, the following three bases were tested with respect to the deprotonation of **3a**–**c**: KHMDS, which was used before [15–17], MeLi and *n*-BuLi, varying in basicity and nature of the counter ion. In particular, the Li cation can be expected to display stronger P–Li and/or N–Li interactions, compared to interactions with the significantly larger K cation.

In contrast to previous studies, the reaction of **3a**–**c** with one equivalent of base in THF did not lead to any of the desired products **M-4a**–**c** or **M-5a**–**c** (Scheme 2). Instead, mixtures of **3a**, **3b** or **3c**, respectively, and several unknown phosphorus compounds were formed. This finding was independent from other reaction conditions, such as temperature and concentration.

Further investigations of **3b** in THF showed that the use of two equivalents of any of the bases mentioned above leads to the N-H deprotonation product **M-4b** (Scheme 2). In the row of bases, KHMDS provided the worst and *n*-BuLi the best result concerning selectivity, which could be tentatively attributed to the highest basicity of the latter. The reaction outcome was temperature independent, and the reaction could also be conducted at room temperature.

To check the effect of a more separated counter cation, two equivalents of a base and two equivalents of the corresponding crown ether were added to a THF solution of **3b** at −80 °C, which resulted in P-H deprotonation, instead, yielding the mono-metalated aminophosphane complex **M-5b** selectively (Scheme 2). The same behaviour in regioselective deprotonation of 1,2-bifunctional complexes could be confirmed by NMR spectroscopy for complexes **3a** and **3c**.

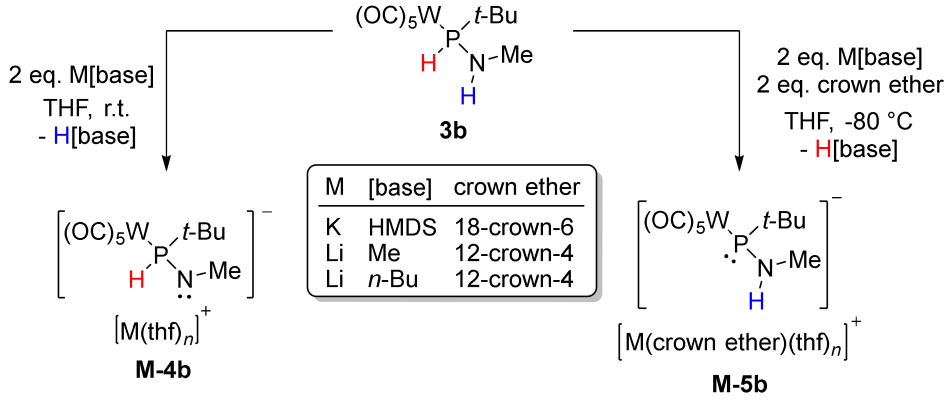

Scheme 2. Regioselective deprotonation of 1,2-bifunctional aminophosphane complex **3b**.

Table 2 contains selected ^{31}P NMR data of the **Li/K-4b** and **Li/K-5b** in THF solution. The comparison of the two metalated derivatives **M-4b** and **M-5b** revealed that their experimentally observed resonances were almost invariant, i.e., there was no clear cation dependency. The values are very close to the computed (GIAO/TPSS-D3/def2-QZVP//CPCM$_{thf}$/TPSS-D3/def2-TZVP$_{ecp}$) values for the respective naked anions, which most likely parallels the occurrence of solvent and/or crown ether separated ion pairs in solution.

Table 2. Selected experimental and calculated NMR data (THF) of species that might result in the deprotonation processes.

	$\delta(^{31}P)$/ppm	$\delta(^{31}P)_{calc}$/ppm[a]	$^{1}J_{W,P}$/Hz	$^{1}J_{P,H}$/Hz
3b	67.3	67.3	238.2	337.0
3f	91.0	86.9	239.5	358.8
Li-4b	49.6	43.6 (**4b**$^-$) 67.9 (**Li-4b**) [b] 69.5 (**thf-Li-4b**) [b] 72.6 (**Li-12c4-4b**) [b]	189.0	310.4
K-4b	48.5	52.3 (**K-4b**) [b] 62.4 (**K-18c6-4b**) [b]	188.8	309
Li-5b	89.9 (br)	95.2 (**5b**$^-$) 87.3 (**thf-Li-12c4-5b**) [b] 68.1 (**Li-12c4-5b**) [b]	- [c]	-
K-5b	89.1	86.3 (**K-5b**) [b] 77.1 (**K-18c6-5b**) [b]	76.1	-
Li-6b	55.0	78.3 (**6b**$^-$) 72.6 (**Li-12c4-6b**) [b]	196.5	-

[a] $\delta(^{31}P)_{calc}$ referenced to **3b**. [b] Compared to naked **4b**$^-$ (43.6 ppm), **5b**$^-$ (95.2 ppm) and **6b**$^-$ (78.3 ppm) anions. [c] Not observed due to broadening of the signal.

In silico, the N- and P-deprotonations of **3b** were computed (CPCM$_{thf}$/PW6B95-D3/def2-QZVP$_{ecp}$//CPCM$_{thf}$/TPSS-D3/def2-TZVP$_{ecp}$) using MeLi as the model in THF (with four explicit molecules), which proceeds exergonically by ΔE_{ZPE} = −47.07 or −53.07 kcal/mol (ΔG = −11.13 or −17.63 kcal/mol), respectively, with the formation of methane and the $[Li(thf)_4]^+$ salts of **4b**$^-$ and **5b**$^-$ anions. The higher thermodynamic stability of **5b**$^-$ arises from the delocalization of the negative charge over the neighbouring metal fragment. Moreover, the anionic N-centre in **4b**$^-$ donates electron density into the P–N bond yielding double bond character with an MBO$_{P\text{-}N}$ of 1.66, an effect that was not observed the other way around in **5b**$^-$ with an MBO$_{P\text{-}N}$ of just 0.96. The SOPT (second order perturbation theory) analysis in NBO basis for **4b**$^-$ unveils a remarkable electron donation from the σ(P-H) to the π*(P=N) orbital and from the π*(P=N) to the σ*(P-H) orbital

(amounting to 100.66 and 19.95 kcal/mol, respectively), which would explain the destabilization of the P–H bond in **4b**$^-$ with an $MBO_{P\text{-}H}$ of 0.84, in comparison with **3f** $MBO_{P\text{-}H}$ of 0.95. The latter may further enhance the formation of **5b**$^-$ from **4b**$^-$ and, therefore, **7b** in the end. Coordination to the K cation shows little influence on the P–N/P–H bonding situation in **4b**$^-$ with $MBO_{P\text{-}N}$ 1.50 and $MBO_{P\text{-}H}$ 0.88.

The ^{31}P resonances of the amide complexes **M-4b** were found to be 20 ppm highfield-shifted compared to **3b** and showed significantly decreased $^1J_{W,P}$ and $^1J_{P,H}$ coupling constant magnitudes. This trend is in accordance with the observations made earlier for the *P*-CPh_3 substituted derivative [16]. As shown by the calculations (*vide supra*), N-H deprotonation significantly strengthens the PN bond, which weakens the other phosphorus bonds and decreases the respective *J* values (**4b**$^-$**:** MBO_{PN} 1.66; **3b:** MBO_{PN} 1.08). The significant decrease in the $^1J_{P,C}$ coupling constant to 20.8 Hz in **Li-4b** from 28.3 Hz in **3b** is in line with these findings.

Li-4b could be isolated as a yellow solid, which was very sensitive towards air and moisture. It decomposed over hours in solution and in the solid state, even under inert atmosphere, reforming the starting material, but also leading to two unknown phosphorus compounds ($\delta(^{31}P)$/ppm = 71.5 ($^1J_{W,P}$ = 233 Hz, $^1J_{P,H}$ = 338 Hz), 89.8 (no detectable Table 1 $J_{W,P}$, $^1J_{P,H}$ = 278 Hz)). The $^{13}C\{^1H\}$ NMR spectrum of **Li-4b** showed a 10 to 20 ppm downfield shift of the CO resonance signals, which fits with an increased electron density in the PN bond. In comparison to **3b**, all ^{1}H NMR resonance signals of **Li-4b** were approximately 0.4 ppm downfield-shifted. Remarkably, the ^{1}H NMR spectrum also revealed the presence of one THF molecule in the complex, which remained after washing and drying. Therefore, it seems to be tightly bound to the lithium cation (*vide infra*) and to be necessary for the stabilization (calculated Li-O distance in **Li(thf)-4b** of 1.91 Å, with $MBO_{Li\text{-}O}$ 0.56). In the FT-IR spectrum of **Li-4b,** the N-H vibration mode was not present and, hence, confirmed the proposed composition.

The ^{31}P resonance signals of **M-5b** are 20 ppm downfield-shifted in comparison to **3b**, in general, which is in accordance to previously observed M/N(H)R phosphinidenoid complexes [15–17]. In addition, the $^1J_{W,P}$ coupling constant has a characteristically small value [12–19]. Presumably related to the decomposition of crown ethers in basic media at ambient temperatures, **M-5b** turned out to be thermally unstable and could not be further characterized, in contrast to previous studies, which even allowed for the isolation of a K/N(H)R phosphinidenoid complex [16,17], but not for the isolation of the corresponding amide complex. Upon warming up, **M-5b** decomposed, providing first the amide complex **M-4b** and, afterwards, a mixture of four not further characterized main products, displaying signals in the ^{31}P NMR spectrum at 41.9 ppm (no $J_{W,P}$, no $^1J_{P,H}$), 86.1 ppm ($^1J_{W,P}$ = 226 Hz), 91.5 ppm ($^1J_{W,P}$ = 230 Hz, $^1J_{P,H}$ = 276 Hz) and 99.8 ppm ($^1J_{W,P}$ = 228 Hz, $^1J_{P,H}$ = 283 Hz) (see ESI).

However, the presence of **Li-5b** in solution could be further proven by a follow-up reaction with MeI as an electrophile and giving rise to the expected *P*-methylated complex **7b,** possessing a resonance at 70.7 ppm ($^1J_{W,P}$ = 252.0 Hz) (Scheme 3). Due to its similarity to the aminophosphane complex **3b,** the analytical data do not differ too much, except for those corresponding to the missing PH unit, such as the vibration mode in the FT-IR spectrum.

Interestingly, also the reaction of **Li-4b** with MeI yielded the same product **7b**, and not the expected N-methylation product **3f**. For **7b** to form from both compounds **Li-4b** and **Li-5b**, a proton transfer has to occur in the former, which will be discussed below. The ^{31}P NMR spectroscopic reaction monitoring of the formation of **7b** showed an intermediate that displayed a ^{31}P resonance signal at 55.0 ppm without a $^1J_{P,H}$ coupling and a $^1J_{W,P}$ coupling of 196.5 ppm, being somehow similar to values of the amide complexes **M-4b**. Based on these observations, the structure of this intermediate can be tentatively assigned to the *P*-methylated amide complex **6b** (cf. Scheme 3). Intermediate **6b** and compound **7b** are initially formed in a ratio of 86:14 (at room temperature), while after 4.5 h, it changed to

23:77, with solely **7b** remaining in the end (see ESI). The existence of a dianionic complex, bearing neither a P-H nor a N-H function, was excluded based on the ^{31}P NMR parameter.

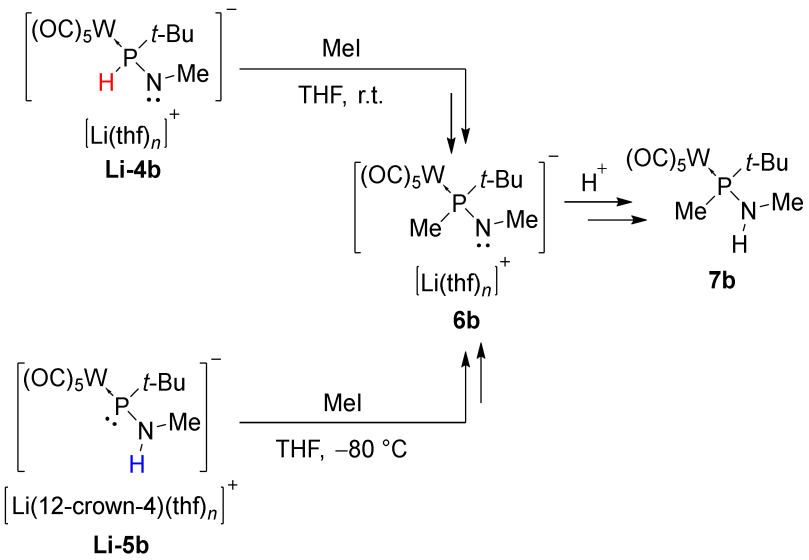

Scheme 3. Reactions of *P*-amido complex **Li-4b** and phosphinidenoid complex **Li-5b** with MeI as the electrophile, yielding complex **7b** as the final product in both cases.

3.3. Theoretical Investigations on the Mechanism

To further unveil the very surprising formation of **7b** in both methylation reactions and particularly from **Li-4b** (Scheme 4), quantum chemical calculations were performed. As stated beforehand, initial N-coordination of the solvated MeLi reagent favours N-deprotonation of **3b** to afford complexes **Li(thf)-4b** or **Li(thf)$_2$-4b**, used here merely as simplified models of Li-coordinated amide salts. Noteworthy is the higher stability of the former, bearing only one THF molecule bound, despite featuring a less coordinatively saturated Li^+ cation, in agreement with the experimental observations (*vide supra*). Formation of the Li(thf)$_2$I adduct of the final product, **[Li(thf)$_2$I]7b**, could proceed through (barrierless) *P*-methylation of **Li^N(thf)$_2$-5b**, but this would require the P-to-N hydrogen shift in **Li(thf)$_2$-4b**, which is kinetically hampered ($\Delta\Delta E_{ZPE}^{\ddagger}$ = 55.23 kcal/mol), as in the above-mentioned case of the naked anions (**4b**$^-$ → **5b**$^-$). A somewhat lower barrier ($\Delta\Delta E_{ZPE}^{\ddagger}$ = 50.64 kcal/mol) was obtained by an additional explicit THF molecule-assisted hydrogen shift (see ESI). A lower energy path would produce **[Li(thf)$_2$I]7b** through tungsten-methylation of **Li(thf)$_2$-4b**, W-to-P methyl group shift (reductive coupling), lower barrier P-to-N trans-protonation ($\Delta\Delta E_{ZPE}^{\ddagger}$ = 42.43 kcal/mol) and P-complexation (Scheme 4). However, we assume that the tentatively proposed PH group-lacking intermediate **6b** is indeed **Li(thf)$_2$-5b^N**, whose formation could be alternatively explained not via intra- but intermolecular trans-protonation (not computed) from **Li(thf)$_2$-4b**.

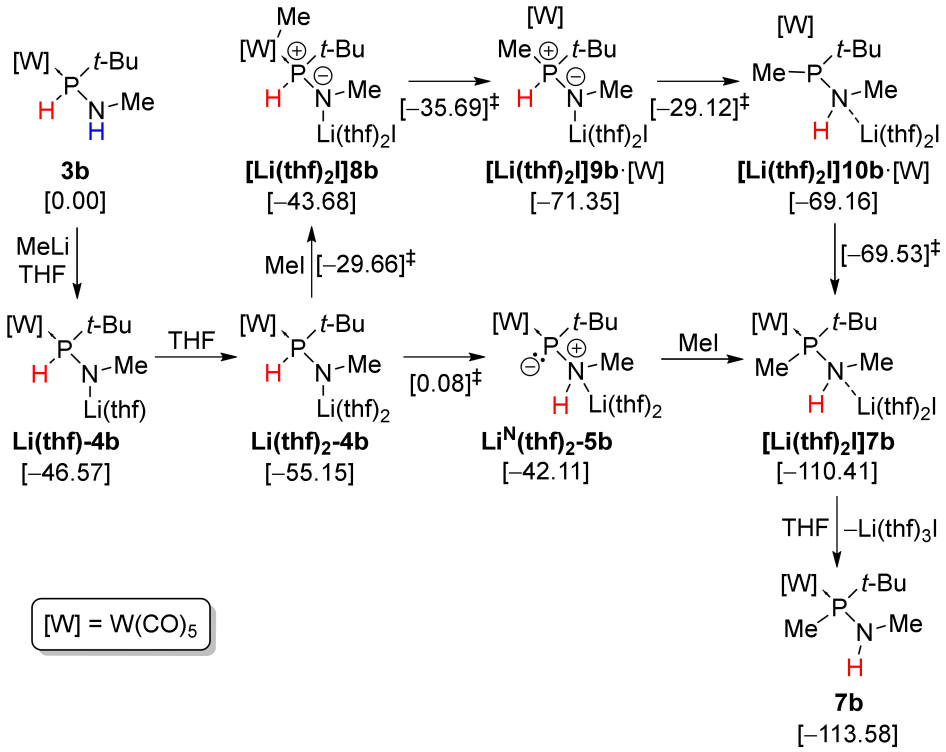

Scheme 4. Mechanistic proposal for the transformation of aminophosphane complex **3b** into the *P*-methylation product **7b** via *P*-amido complex **Li-4b**. Relative zero point-corrected energies (kcal/mol) are quoted in square brackets.

4. Conclusions

Effective synthesis of 1,2-bifunctional aminophosphane complexes **3a**–**f** was achieved using the reaction of a sterically less demanding Li/Cl phosphinidenoid $W(CO)_5$ complex with ammonia and amines RR'NH. A new M/N(H)Me phosphinidenoid complex **Li-5b** was accessed via selective deprotonation of 1,2-bifunctional aminophosphane complex **3b** using *n*-BuLi as base in presence of 12-crown-4, and the phosphanylamido complex **Li-4b** (Supplementary Materials) was obtained as isolable, but not bottleable product in absence of the crown ether. Subsequent reactions of both **Li-4b** and **Li-5b** with MeI revealed the formation of the same *P*-methylated complex **7b** via a common intermediate **6b**. On the basis of quantum chemical calculations, the observed ^{31}P NMR shifts were assigned to the structures in the solution. Furthermore, insights into P–N and P–H bond strengths were obtained and the preferred path of the solvent separated P-anion $\mathbf{5b}^-$ to form **7b** via the methylation analyzed.

Supplementary Materials: The following supporting information can be downloaded at: https://www.mdpi.com/article/10.3390/org3030013/s1, Figure S1: NMR spectra of complex **3a**; Figure S2: NMR spectra of complex **3b**; Figure S3: NMR spectra of complex **3c**; Figure S4: NMR spectra of complex **3d**; Figure S5: NMR spectra of complex **3e**; Figure S6: NMR spectra of complex **3f** in product mixture; Figure S7: NMR spectra of compound **Li-4b** in product mixture; Figure S8: NMR spectra of compound **Li-5b** in reaction mixture; Figure S9: NMR spectra of compound **K-5b** in reaction mixture; Figure S10: NMR spectra of compound **7** in product mixture; Figure S11: Decomposition of **Li-5b** in THF solution on warming up from −80 °C; Figure S12: NMR spectra measured for the reaction of **3b** with MeLi in presence of 12-crown-4 and *n*-BuLi, followed by treatment with MeI; Cartesian coordinates and energies for all computed species; Table S1: Computed ^{31}P chemical shifts (in ppm).

Author Contributions: Conceptualization, A.E.F. and R.S.; methodology, validation and formal analysis, T.T.; investigation, T.T., P.J. and A.S.; resources, A.E.F. and R.S.; data curation, A.E.F. and R.S.; writing—original draft preparation, including review and editing, A.E.F. and R.S.; supervision, R.S.; project administration, R.S.; funding acquisition, R.S. All authors have read and agreed to the published version of the manuscript.

Funding: This research was funded by the Deutsche Forschungsgemeinschaft, grant number STR 411/26-3 and STR 411/46-1.

Data Availability Statement: Data supporting the reported results can be found in the ESI.

Acknowledgments: We are grateful to Stefan Grimme in combination with the Mulliken Center (University of Bonn) and the *Servicio de Cálculo Científico* (University of Murcia) for technical support and the computational resources.

Conflicts of Interest: The authors declare no conflict of interest.

References

1. Harris, G.S. The Reaction of Chloro(bistrifluoromethyl)phosphine with Amines and Ammonia. *Proc. Chem. Soc.* **1957**, *105–128*, 118–119. [CrossRef]
2. Burg, A.B.; Slota, P.J. Dimethylaminodimethylphosphine. *J. Am. Chem. Soc.* **1958**, *80*, 1107–1109. [CrossRef]
3. Sisler, H.; Smith, N. Some N-Substituted Aminodiphenylphosphines. *J. Org. Chem.* **1961**, *26*, 611–613. [CrossRef]
4. Atkinson, L.K.; Smith, D.C. Molybdenum carbonyl complexes of (dialkylamino)-diphenylphosphines (R_2NPPh_2). *J. Organomet. Chem.* **1971**, *33*, 189–194. [CrossRef]
5. Kroshefsky, R.D.; Verkade, J.G.; Pipal, J.R. Coordination properties of constrained aminophosphanes. *Phosphorus Sulfur Relat. Elem.* **1979**, *6*, 377–389. [CrossRef]
6. Huttner, G.; Müller, H.-D. Stabilization of Unknown Phosphanes: Secondary Amino- and Alkoxyphosphanes as Complex Ligands. *Angew. Chem. Int. Ed. Engl.* **1975**, *14*, 571–572. [CrossRef]
7. Marinetti, A.; Mathey, F. Stabilization of R-P(H)A species (A = OH, OR, S, NH_2, NHR, NR_2, Cl, Br, I) by complexation with chromium and tungsten pentacarbonyls. *Organometallics* **1982**, *1*, 1488–1492. [CrossRef]
8. Mathey, F. Phospha-Organic Chemistry: Panorama and Perspectives. *Angew. Chem. Int. Ed. Engl.* **2003**, *42*, 1578–1604. [CrossRef]
9. Wit, J.B.M.; de Jong, G.B.; Schakel, M.; Lutz, M.; Ehlers, A.W.; Slootweg, J.C.; Lammertsma, K. iPr_2N–P=$Fe(CO)_4$ in Olefinic Solvents: A Reservoir of a Transient Phosphinidene Complex Capable of Substrate Hopping. *Organometallics* **2016**, *35*, 1170–1176. [CrossRef]
10. Niecke, E.; Ringel, G. Synthesis of a secondary aminophosphine. *Angew. Chem. Int. Ed. Engl.* **1977**, *16*, 486–487; Erratum in *Angew. Chem.* **1977**, *89*, 501–502. [CrossRef]
11. Niecke, E.; Rüger, R. Bis(trimethylsilyl)aminophosphane. *Angew. Chem. Int. Ed. Engl.* **1982**, *21*, 62–71. [CrossRef]
12. Duan, L.; Schnakenburg, G.; Daniels, J.; Streubel, R. P-OR functional phosphanido and/or Li/OR phosphinidenoid complexes? *Eur. J. Inorg. Chem.* **2012**, *2012*, 3490–3499. [CrossRef]
13. Junker, P.; Qu, Z.-W.; Kalisch, T.; Schnakenburg, G.; Espinosa Ferao, A.; Streubel, R. A case study on the conversion of Li/Cl phosphinidenoid into phosphinidene complexes. *Dalton Trans.* **2021**, *50*, 739–745. [CrossRef] [PubMed]
14. Schmer, A.; Volk, N.; Espinosa Ferao, A.; Streubel, R. Access and unprecedented reaction pathways of Li/Cl phosphinidenoid iron(0) complexes. *Dalton Trans.* **2019**, *48*, 339–345. [CrossRef] [PubMed]
15. Majhi, P.K.; Kyri, A.W.; Schmer, A.; Schnakenburg, G.; Streubel, R. Synthesis and deprotonation of aminophosphane complexes: Potassium phosphinidenoid complexes and a new synthetic protocol for complexes with three-membered P-ring ligands. *Chem. Eur. J.* **2016**, *22*, 15413–15419. [CrossRef]
16. Streubel, R.; Schmer, A.; Kyri, A.W.; Schnakenburg, G. 1,1′-Bifunctional Aminophosphane Complexes via N–H Bond Insertions of a Li/Cl Phosphinidenoid Complex and First Studies on N/P Mono Functionalizations. *Organometallics* **2017**, *36*, 1488–1495. [CrossRef]
17. Schmer, A.; Terschüren, T.; Schnakenburg, G.; Espinosa Ferao, A.; Streubel, R. Access to 1,1′-Bifunctional Phosphane Iron(0) Complexes via P-N Bond-Forming Reactions and Selective P-Functionalizations. *Eur. J. Inorg. Chem.* **2019**, *2019*, 1604–1611. [CrossRef]
18. Schmer, A.; Junker, P.; Espinosa Ferao, A.; Streubel, R. M/X Phosphinidenoid Metal Complex Chemistry. *Acc. Chem. Res.* **2021**, *54*, 1754–1765. [CrossRef]
19. Streubel, R.; Kyri, A.W.; Duan, L.; Schnakenburg, G. Synthesis of Li/OR phosphinidenoid complexes: On the evidence for intramolecular O–Li donation and the effect of cation encapsulation. *Dalton Trans.* **2014**, *43*, 2088–2097. [CrossRef]
20. Tolman, C.A. Steric effects of phosphorus ligands in organometallic chemistry and homogeneous catalysis. *Chem. Rev.* **1977**, *77*, 313–348. [CrossRef]
21. Marinetti, A.; Bauer, S.; Ricard, L.; Mathey, F. The "Phospha-Wittig" Reaction: A New Method for Building Phosphorus Carbon Double and Single Bonds from Carbonyl Compounds. *Organometallics* **1990**, *9*, 793–798. [CrossRef]
22. Neese, F. The ORCA program system. *Wiley Interdiscip. Rev. Comput. Mol. Sci.* **2012**, *2*, 73–78. [CrossRef]

23. Tao, J.; Perdew, J.P.; Staroverov, V.N.; Scuseria, G.E. Climbing the Density Functional Ladder: Nonempirical Meta–Generalized Gradient Approximation Designed for Molecules and Solids. *Phys. Rev. Lett.* **2003**, *91*, 146401. [CrossRef] [PubMed]
24. Grimme, S.; Antony, J.; Ehrlich, S.; Krieg, H. A consistent and accurate ab initio parametrization of density functional dispersion correction (DFT-D) for the 94 elements H-Pu. *J. Chem. Phys.* **2010**, *132*, 154104–154119. [CrossRef] [PubMed]
25. Grimme, S.; Ehrlich, S.; Goerigk, L. Effect of the damping function in dispersion corrected density functional theory. *J. Comput. Chem.* **2011**, *32*, 1456–1465. [CrossRef]
26. Weigend, F.; Häser, M.; Patzelt, H.; Ahlrichs, R. RI-MP2: Optimized auxiliary basis sets and demonstration of efficiency. *Chem. Phys. Lett.* **1998**, *294*, 143–152. [CrossRef]
27. Weigend, F.; Ahlrichs, R. Balanced basis sets of split valence, triple zeta valence and quadruple zeta valence quality for H to Rn: Design and assessment of accuracy. *Phys. Chem. Chem. Phys.* **2005**, *7*, 3297–3305. [CrossRef]
28. Weigend, F.; Furche, F.; Ahlrichs, R. Gaussian basis sets of quadruple zeta valence quality for atoms H–Kr. *J. Chem. Phys.* **2003**, *119*, 12753–12762. [CrossRef]
29. Eichkorn, K.; Weigend, F.; Treutler, O.; Ahlrichs, R. Auxiliary basis sets for main row atoms and transition metals and their use to approximate Coulomb potentials. *Theor. Chem. Acc.* **1997**, *97*, 119–124. [CrossRef]
30. Weigend, F. Accurate Coulomb-fitting basis sets for H to Rn. *Phys. Chem. Chem. Phys.* **2006**, *8*, 1057–1065. [CrossRef]
31. Deglmann, P.; May, K.; Furche, F.; Ahlrichs, R. Nuclear second analytical derivative calculations using auxiliary basis set expansions. *Chem. Phys. Lett.* **2004**, *384*, 103–107. [CrossRef]
32. Zhao, Y.; Truhlar, D.G. Design of Density Functionals That Are Broadly Accurate for Thermochemistry, Thermochemical Kinetics, and Nonbonded Interactions. *J. Phys. Chem. A* **2005**, *109*, 5656–5667. [CrossRef] [PubMed]
33. Schreckenbach, G.; Ziegler, T. Calculation of NMR Shielding Tensors Using Gauge-Including Atomic Orbitals and Modern Density Functional Theory. *J. Phys. Chem.* **1995**, *99*, 606–611. [CrossRef]
34. Fassbender, J.; Schnakenburg, G.; Espinosa Ferao, A.; Streubel, R. Effects of diminished steric protection at phosphorus on stability and reactivity of oxaphosphirane complexes. *Dalton Trans.* **2018**, *47*, 9347–9354. [CrossRef] [PubMed]
35. Müller, T.E.; Mingos, D.M.P. Determination of the Tolman cone angle from parameters and a statistical analysis using the Data Base. *Transit. Met. Chem.* **1995**, *20*, 533–539. [CrossRef]